1521-0111/85/1/139–147$25.00
MOLECULAR PHARMACOLOGY

http://dx.doi.org/10.1124/mol.113.088914
Mol Pharmacol 85:139–147, January 2014

Regulation of Intestinal Cytochrome P450 Expression by Hepatic Cytochrome P450: Possible Involvement of Fibroblast Growth Factor 15 and Impact on Systemic Drug Exposure

Yi Zhu, Xinxin Ding, Cheng Fang, and Qing-Yu Zhang

Laboratory of Molecular Toxicology, Wadsworth Center, New York State Department of Health, and School of Public Health, State University of New York at Albany, Albany, New York

Received August 2, 2013; accepted November 1, 2013

ABSTRACT

Tissue-specific deletion of the gene for NADPH-cytochrome P450 (P450) reductase (CPR), the essential electron donor to all microsomal P450 enzymes, in either liver or intestine, leads to upregulation of many P450 genes in the tissue with the *Cpr* deletion. Here, by studying the liver-specific *Cpr*-null (LCN) mouse, we examined whether an interorgan regulatory pathway exists, such that a loss of hepatic CPR would cause compensatory changes in intestinal P450 expression and capacity for first-pass metabolism of oral drugs. We show for the first time that intestinal expression of CYP2B, 2C, and 3A proteins was increased in LCN mice by 2- to 3-fold compared with wild-type (WT) mice, accompanied by significant increases in small intestinal microsomal lovastatin-hydroxylase activity and systemic clearance of oral lovastatin (at 5 mg/kg). Additional studies showed that the hepatic *Cpr* deletion, which caused large decreases in bile acid (BA) levels in the liver, intestine, plasma, and intestinal content, led to drastic decreases in the mRNA levels of intestinal fibroblast growth factor 15 (FGF15), a target gene of the BA receptor farnesoid X receptor. Furthermore, treatment of mice with FGF19 (the human counterpart of mouse FGF15) abolished the difference between WT and LCN mice in small intestinal (SI) CYP3A levels at 6 hours after the treatment. Our findings reveal a previously unrecognized direct role of intestinal FGF15/19 in the regulation of SI P450 expression and may have profound implications for the prediction of drug exposure in patients with compromised hepatic P450 function.

Introduction

Generally, the liver, with its abundant cytochrome P450 (P450) enzymes, is the major metabolic organ; in most cases, the loss of hepatic P450 function will lead to reduced rates of clearance of drugs or toxicants, as has been demonstrated in a mouse model with liver-specific deletion of the NADPH-cytochrome P450 reductase (*Cpr*) gene (Gu et al., 2003; Zhang et al., 2007; Fang et al., 2008), designated liver-*Cpr*-null (LCN). However, for oral drugs, small intestinal (SI) epithelial cells (enterocytes) serve as the first metabolic site. Those drugs surviving the first-pass metabolism in the SI will undergo further extraction in the liver before they reach systemic circulation. Therefore, P450 enzymes in the SI as well as those in the liver play essential roles in controlling the systemic exposure of oral drugs, as we have demonstrated for nifedipine and lovastatin (LVS) (Zhang et al., 2009; Zhu et al., 2011) using an intestinal epithelium (IE)-*Cpr*-null mouse model (Zhang et al., 2009), in which the *Cpr* gene is specifically deleted in the intestinal epithelium.

This work was supported in part by the National Institutes of Health National Institute of General Medical Sciences [Grant GM082978].
dx.doi.org/10.1124/mol.113.088914.

The importance of hepatic and intestinal P450 enzymes to the maintenance of endogenous homeostasis and the protection against orally ingested xenobiotic compounds is illustrated by the compensatory increases in the expression of most xenobiotic metabolizing P450s, such as CYP2B, 2C, and 3A, in the organ (liver or SI) that has lost microsomal P450 function as a result of the tissue-specific *Cpr* deletion (Gu et al., 2003; Henderson et al., 2003; Zhang et al., 2009). Given the common and sequential role of the SI and liver in the first-pass metabolism of ingested xenobiotics, it is plausible that the loss of P450 function in one organ may also cause compensatory increases in P450 expression in the other organ. This scenario has so far been found true in the IE-*Cpr*-null mice for only one P450, CYP1A1, the expression of which was upregulated in not only the SI, but also in the liver, lung, and kidney of the IE-*Cpr*-null mice (Zhang et al., 2009). Microarray analysis of the liver of IE-*Cpr*-null mice revealed minimal changes in gene expression (J. D'Agostino and Q.-Y. Zhang, unpublished data), a result suggesting that, at least in mice kept in the laboratory setting, the liver has sufficient reserve capacity to deal with the increased tissue burden of dietary chemicals and compounds reabsorbed after enterohepatic recirculation, on the loss of intestinal P450 function. However, it remains to be determined

ABBREVIATIONS: ASBT, ileal apical sodium bile transporter; BA, bile acids; CA, cholic acid; CAR, constitutive androstane receptor; CPR/POR, NADPH-cytochrome P450 reductase; d4-CA, cholic-2,2,4,4-d4-acid; FGF15, fibroblast growth factor 15; FGF19, fibroblast growth factor 19; FXR, farnesoid X receptor; IE, intestinal epithelium; LC-MS/MS, liquid chromatography–tandem mass spectrometry; LCN, liver-specific *Cpr*-null; LVA, lovastatin hydroxyl acid; LVS, lovastatin; MCA, muricholic acid; P450, cytochrome P450; PBS, phosphate-buffered saline; PXR, pregnane X receptor; SI, small intestine/small intestinal; SHP, small heterodimer partner; SVA, simvastatin; VDR, vitamin D receptor; WT, wild-type.

whether the opposite is true, i.e., whether or not the SI has sufficient capacity to metabolize the increased burden of ingested chemicals and circulating endogenous compounds on the loss of hepatic P450 function or whether or not it will be necessary for the SI to increase levels of P450 expression.

While examining the respective roles of liver and SI P450 enzymes in the first-pass metabolism of several oral drugs (Zhu et al., 2011; Zhu and Zhang, 2012), we made an intriguing observation that the clearance of oral LVS was not decreased (at 25 mg/kg), or even increased (at 5 mg/kg), in the LCN mice, which led to the hypothesis that SI LVS metabolism and P450 expression are upregulated by the loss of hepatic P450 function. After successful validation of this hypothesis using LCN mice compared with wild-type (WT) mice, we further explored the mechanisms that underlie the interorgan "cross-talk" by examining the bile acid (BA) pool and expression of BA target genes in the SI. In that connection, BA synthesis in the liver is blocked in mice with liver-specific *Cpr* deletion, leading to reductions in BA levels and bile volume (Henderson, et al., 2003; Weng et al., 2005). Thus, we hypothesized that the alterations in BA signaling in LCN mice led to upregulation of SI P450 expression and function. Our studies showed for the first time that the loss of hepatic CPR/P450 function leads to drastic decreases in the intestinal expression of fibroblast growth factor 15 (FGF15), a BA-induced intestinal hormone that is known to regulate BA homeostasis via inhibition of hepatic *Cyp7a1* gene transcription (Inagaki et al., 2005) and that the upregulation of SI CYP3A expression can be blocked by treatment of mice with FGF19, the human counterpart of mouse FGF15.

Materials and Methods

LVS, lovastatin hydroxyl acid (LVA), and simvastatin (SVA) were purchased from Cayman Chemical (Ann Arbor, MI). NADPH, cholic acid (CA), and taurocholic acid were purchased from Sigma-Aldrich (St. Louis, MO). Cholic-2,2,4,4-d4-acid (d4-CA) was obtained from C/D/N Isotopes (Pointe-Claire, QC, Canada), α- and β-muricholic acid (MCA) and tauro-β-muricholic acid (T-β-MCA) sodium salt were obtained from Steraloids (Newport, RI). All solvents (acetonitrile, methanol, and water) were of high-performance liquid chromatography grade (ThermoFisher Scientific, Waltham, MA). Western blotting reagents were from Life Technologies (Grand Island, NY). Recombinant human fibroblast growth factor 19 (FGF19) was purchased from R&D systems (Minneapolis, MN).

Animals and Treatments. Male and female LCN (Gu et al., 2003) mice (3 to 4 months old) and age-matched WT littermates were used. Animals were given food and water ad libitum. For LVS administration, female WT and LCN mice were given a bolus dose of LVS [dissolved in dimethylsulfoxide/Tween-80/phosphate-buffered saline (PBS) (1:2:7, v/v/v) at 0.5, 2.5 or 5 mg/ml, respectively], via oral gavage (at 5, 10, 25, and 50 mg/kg). For FGF19 treatment, male WT and LCN mice were injected with recombinant human FGF19 (150 μg/kg, dissolved in PBS) through the tail vein; all animals were sacrificed 6 hours later for tissue collection and microsome or RNA preparation. All animal studies were approved by the Institutional Animal Care and Use Committee of the Wadsworth Center.

For the analysis of age-dependent CYP3A expression, tissues from male mice at different ages (17 days, 1 month, and 3 months) were obtained for microsomal preparation. For analysis of CYP3A expression in different SI segments, tissues were taken from the proximal (the first 10 cm from the pyloric sphincter), middle (the middle 10 cm of the jejunum), and distal (10 cm from ileocecal junction) parts of adult male mice.

Isolation of Intestinal Epithelial Cells and Preparation of Microsomes. Tissues from two to three mice were combined for each microsomal preparation. Epithelial cells from the SI were isolated, and microsomal samples were prepared, as described (Zhang et al., 2009). Liver microsomes were prepared essentially as previously reported (Fasco et al., 1993). Microsomal protein concentrations were determined with the bicinchoninic acid protein assay kit (Pierce, Rockford, IL), with bovine serum albumin as the standard. Microsomes were stored at −80°C until use.

Immunoblot Analysis. Microsome proteins were resolved on 10% NuPAGE Bis-Tris gels (Life Technologies, Grand Island, NY) and then transferred to nitrocellulose membranes. For immunodetection, polyclonal rabbit anti-CYP3A1 (Biomol Research Laboratories, Plymouth Meeting, PA) and polyclonal goat anti-rat CYP2B or CYP2C (BD Gentest, Woburn, MA) were used. Peroxidase-labeled goat anti-rabbit IgG and rabbit anti-goat IgG (Sigma-Aldrich) were used as secondary antibodies. The signal was detected with an enhanced chemiluminescence kit (GE Healthcare, Piscataway, NJ), and immunoblot quantification was carried out using a GS-710 Calibrated Imaging Densitometer or a ChemiDoc XRS+ System (Bio-Rad, Hercules, CA). Levels of calnexin were routinely determined as a loading control, with use of a rabbit anti-calnexin antibody (GenScript, Piscataway, NJ).

In Vitro Metabolism of LVS. The assay for microsomal metabolism of LVS and the liquid chromatography–tandem mass spectrometry (LC-MS/MS) analysis for determination of its two metabolites (6′β-hydroxy LVS and 6′-exomethylene LVS) were performed as described (Zhu et al., 2011). Control experiments were performed in which NADPH was omitted. SVA (10 ng in 10 μl acetonitrile/water, v/v, 4/1) was added as an internal standard for monitoring extraction efficiency. For quantitation, LVS was used as a surrogate for construction of calibration curves (with SVA as the internal standard), and relative activities in different microsomal preparations were determined.

Pharmacokinetic Analysis. Mice (LCN and WT, female, five to six in each group) were treated with LVS via oral gavage. Blood samples were collected from the tail vein at 0.25, 0.5, 1, 1.5, 2, and 4 hours after LVS administration. Note that LVS, a lactone prodrug, is quickly converted via hydrolysis to LVA, the active drug in vivo (Duggan et al., 1989) and that LVA, the major circulating form of the drug in mice (Lodge et al., 2008), was determined for LVS pharmacokinetics studies. Both LVS and LVA are CYP3A substrates (Ishigami et al., 2001). The extraction and LC-MS/MS analysis of LVA were performed as described (Zhu et al., 2011). Pharmacokinetic parameters were calculated by noncompartmental analysis using the PK Solver software (in Microsoft Excel). Clearance was calculated as the hybrid constant CL/F, given that bioavailability (F) is not known. Statistical significance of differences between groups was examined using Student's t test.

LC-MS/MS Analysis of BAs. Quantitative analysis of BAs was performed as described previously (Zhang et al., 2013) using an ABI 4000 Q-Trap LC-MS/MS system (Applied Biosystems, Foster City, CA) fitted with a 3.5-μm Symmetry-C18 column (2.1 × 150 mm; Waters, Milford, MA). Calibration curves were constructed using authentic compounds added to charcoal-stripped bovine serum (Hyclone, Logan, UT), and d4-CA was used as an internal standard.

RNA Isolation and Real-Time RNA Polymerase Chain Reaction. Total RNA was prepared from enterocytes and liver of individual LCN and WT mice (three or four in each group, male) using TRIzol (Invitrogen, Carlsbad, CA) essentially as described (Zhang et al., 2003). RNA concentration and purity were determined spectrally, and the integrity of the RNA samples was assessed by ethidium bromide staining after agarose gel electrophoresis. Real-time RNA polymerase chain reaction was performed as described (D'Agostino et al., 2012) using 2 μg of total RNA. The primers used were farnesoid X receptor (FXR) forward, 5′-ccaacctgggtttctaccc-3′, and reverse, 5′-cacacagctcatccccttt-3′ (Cariou et al., 2006); pregnane X receptor (PXR) forward, 5′-caaggccaatggctacca-3′, and reverse, 5′-cgggtgatctcgcaggtt-3′ (Trousson et al., 2009); constitutive androstane receptor (CAR) forward, 5′-ggagcggctgtggaaatattgcat-3′, and reverse, 5′-tccatcttgtagcaaagaggccca-3′

(Patel et al., 2007); vitamin D receptor (VDR) forward, 5′-ttcatcatgccaatgccaatgtccac-3′, and reverse, 5′-gttcacctgccccttcaat-3′ (Froicu et al., 2006); FGF15 forward, 5′-gaggaccaaaacgaacgaaatt-3′, and reverse, 5′-acgtccttgatggcaatcg-3′; small heterodimer partner (SHP) forward, 5′-cgatcctcttcaacccagatg-3′, and reverse, 5′-agggctccaagacttcacaca-3′; CYP7A1 forward, 5′-agcaactaaacaacctgccagtacta-3′, and reverse, 5′-gtccggatattcaaggatgca-3′ (Inagaki et al., 2005); ileal bile acid-binding protein forward, 5′-ggtcttccaggagacgtgat-3′, and reverse, 5′-acattctttgccaatggtga-3′ (Kim et al., 2007); ileal apical sodium bile transporter (ASBT) forward, 5′-tgggtttcttcctggctagact-3′, and reverse, 5′-tgttctgcattccagtttccaa-3′ (Miyata et al., 2011), and CYP3A11 forward, 5′-gacaaacaagcagggatgg-3′, and reverse, 5′- aatgtgggggacagcaaag-3′ (Zhang et al., 2003). The levels of target gene mRNAs in various total RNA preparations were normalized by the level of GAPDH mRNA in a given sample.

Mouse SI Explant Culture. The method for tissue culture was essentially as described in a previous report (Schmidt et al., 2010). Briefly, the SI was collected, flushed with PBS to remove the contents, cut open, and then sliced into small segments (approximately 1 × 3 mm). The segments were cultured at 37°C and 95% oxygen for 6 hours in Dulbecco's modified Eagle's medium (containing 4 g/l glucose and L-glutamine; Invitrogen) supplemented with 100 U/ml penicillin and 100 μg/ml streptomycin, 10% fetal bovine serum, with or without FGF19 (200 ng/ml). After 6 hours, the epithelial cells were harvested and RNA was prepared as described above.

Results

Effects of Hepatic *Cpr* Deletion on P450 Expression in Mouse Intestine. To investigate whether *Cpr* deletion in the liver has any impact on P450 expression in the SI, we first compared SI levels of CYP3A enzymes, one of the major subfamily of drug-metabolizing P450s, between LCN and WT mice. CYP3A protein expression levels in liver, lung, and kidney were also determined. As shown in Fig. 1A, upregulation of CYP3A expression was evident in hepatic microsomal samples of LCN mice (by ~3-fold), as previously reported (Gu et al., 2003). Surprisingly, an increase in CYP3A expression was also found in SI (by ~2-fold), but not in lung or kidney, of LCN mice, relative to WT mice. This compensatory induction of intestinal CYP3A expression was confirmed to occur in both male and female LCN mice and in both SI and colon (data not shown).

We further examined whether the intestinal expression of CYP2B and 2C, two other subfamilies of major-drug-metabolizing P450 enzymes, is affected by hepatic *Cpr* deletion. As shown in Fig. 1B, levels of CYP2B and 2C in the SI were elevated (by 2- to 3-fold) in the LCN mice, compared with WT mice. Of note, the anti-P450 antibodies were all polyclonal and are expected to recognize multiple, if not all, members in the CYP2B, 2C, or 3A gene subfamilies.

The time course of the effects of hepatic *Cpr* deletion on intestinal CYP3A protein expression was examined by studying mice at different ages (17 days, 1 month, and 3 months). The compensatory increase in CYP3A expression was evident in both 1- and 3-month-old LCN mice, but not in 17-day-old mice, compared with age-matched WT littermates (Fig. 1C). This time course agreed well with the postnatal onset of Cre recombinase expression (and consequent *Cpr* deletion) in the liver of LCN mice (Gu et al., 2003, 2007).

The spatial distribution of the compensatory increase in intestinal CYP3A expression in the LCN mice was also investigated by an examination of CYP3A expression in intestinal epithelial cells taken from the proximal, middle, and distal parts of the SI. As shown in Fig. 1D, microsomal levels of CYP3A protein, which decreased toward the distal end of the SI in both WT and LCN mice, were higher in all three SI segments in the LCN mice compared with corresponding segments in the WT mice (by 2.0-, 2.8- and 1.8-fold, respectively, in proximal, middle, and distal segments).

Impact of Hepatic *Cpr* Deletion on P450-Mediated LVS Metabolism in SI Microsomes. The compensatory increase in CYP3A expression in the SI of the LCN mice was confirmed by measuring in vitro microsomal activities toward LVS, a CYP3A substrate. As shown in Fig. 2, the loss of hepatic CPR expression led to significant decreases in the rates of formation of 6′β-hydroxy LVS and 6′-exomethylene LVS, two major metabolites of LVS, by hepatic microsomes from LCN mice, compared with WT mice. The extent of decrease in hepatic microsomal activity toward LVS (~93%) was similar to that found previously for the metabolism of 4-(methylnitrosamino)-1-(3-pyridyl)-1-butanone and acetaminophen in the LCN mice (>90%) (Gu et al., 2003). In contrast, the rates of LVS metabolite formation were increased, by 200% in SI microsomes from LCN mice compared with those from WT mice.

Impact of Hepatic *Cpr* Deletion on First-Pass Clearance of LVS. Rates of LVS clearance were compared between WT and LCN mice. The pharmacokinetic profiles and parameters are shown in Fig. 3 and Table 1, respectively. At doses of 5 and 10 mg/kg, LVS clearance rates in LCN mice were faster than that in WT mice. At the dose of 5 mg/kg, the area under the curve (AUC_{0-2h}) and C_{max} values were both ~2-fold greater in WT than in LCN mice, whereas the clearance rate was 1.7-fold higher in LCN than in WT mice (Table 1). However, at a dose of 25 mg/kg, there was no difference in pharmacokinetic profiles or parameters between the two mouse strains, whereas at the dose of 50 mg/kg, LVS clearance in LCN mice was actually slower than in WT mice. At 50 mg/kg, the area under the curve (AUC_{0-4h}), C_{max}, and $t_{1/2}$ values were 2.7-, 1.9- and 1.4-fold, respectively, greater, whereas the clearance rate was 2.7-fold lower, in LCN than in WT mice (Table 1).

Effects of Hepatic *Cpr* Deletion on Systemic and Intestinal BA Homeostasis and Expression of BA-Regulated Genes. To test the hypothesis that alterations in BA signaling in the LCN mice led to upregulation of SI P450 expression and function, we first compared BA levels in blood, liver, SI, and intestinal content from WT and LCN mice. It was reported previously that the loss of CPR in the liver leads to reduced hepatic BA production (Henderson et al., 2003; Weng et al., 2005); however, it is not known whether or to what extent BA homeostasis in the intestine is altered. As shown in Fig. 4, the levels of five major murine BAs (CA, taurocholic acid, α-MCA, β-MCA, and T-β-MCA) were all significantly decreased in liver, SI, plasma, and intestinal content of the LCN mice relative to WT littermates.

Real-time RNA polymerase chain reaction experiments were then conducted to compare expression levels of various genes, which can be regulated by BA, in SI epithelial cells of WT and LCN mice. As shown in Fig. 5, although FXR expression was increased ~3-fold in the SI of LCN mice, PXR, CAR, and VDR mRNA levels were not different from those in WT mice. The expression of several FXR target genes was also altered: FGF15, ileal bile acid-binding protein, and SHP levels were all decreased (by 15-, 4- and 5-fold, respectively),

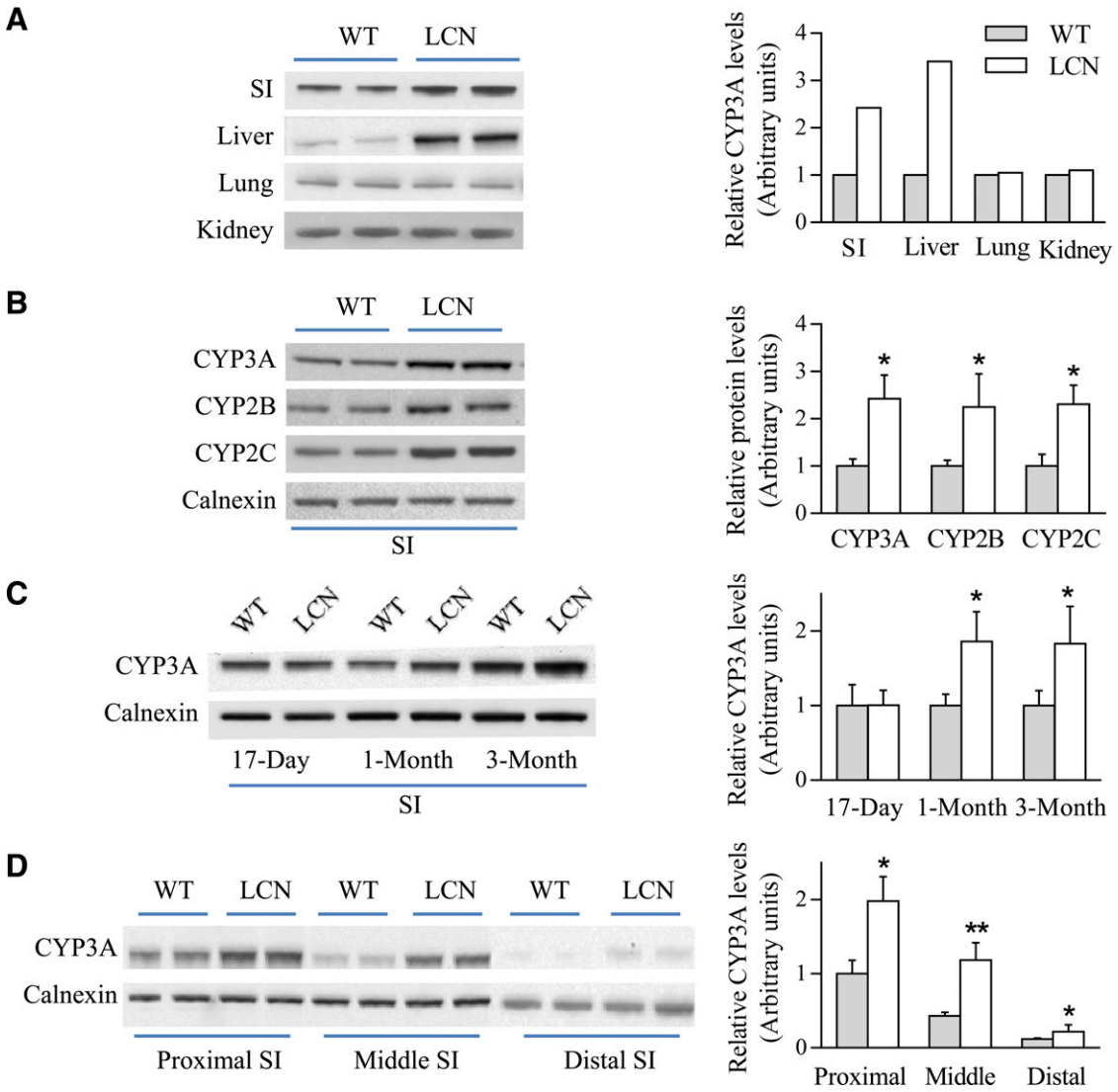

Fig. 1. Immunoblot analysis of P450 expression in WT and LCN mice. (A) Microsomal proteins from SI (20 μg), liver (10 μg), lung (10 μg), and kidney (10 μg) of adult male mice were analyzed in duplicate for CYP3A expression. (B) SI microsomal proteins (10 μg) of adult male mice were analyzed in duplicate on immunoblots for the expression of CYP3A, 2B, and 2C, as well as calnexin (as a loading control). (C) SI microsomal proteins (20 μg) from mice at 17 days, 1 month, or 3 months of age were analyzed for CYP3A expression. (D) Microsomal proteins (20 μg) from different SI segments of adult male mice were analyzed in duplicate for CYP3A expression. Each microsomal sample was prepared from tissues pooled from two to three mice. Results of densitometric analysis (bar graphs) are normalized by calnexin levels in each sample and are shown in arbitrary units. Typical results are shown. $^{*}P < 0.05$; $^{**}P < 0.01$; compared with WT mice (Student's t test).

whereas the level of ASBT, which is negatively regulated by FXR through SHP, was increased (by 3-fold) in the SI of LCN mice relative to WT mice. This pattern of changed expression of FXR target genes is consistent with a reduced activation of FXR by BAs. The expression of several PXR and CAR target genes, including interferon-γ, intercellular adhesion molecule, aldehyde dehydrogenase 1A1, glutathione *S*-transferase mu 1 and p 1, was also examined, but the results did not show any significant difference in expression levels between the two mouse strains (data not shown).

Effects of FGF15/19 on Intestinal CYP3A Expression in WT and LCN Mice. The upregulation of CYP3A expression in the SI of LCN mice does not seem to involve activation of PXR, CAR, and/or VDR, which are known to be capable of activating CYP3A expression, given the decrease (rather than increase) in SI BA levels (Fig. 4B) and the absence of an increased PXR, CAR, or VDR expression (Fig. 5A). However, a role for the FXR target gene FGF15 is plausible, given its known ability to suppress CYP7A1 expression in the liver, although nothing is known about its ability to regulate intestinal P450 expression. We speculated that the large reduction in FGF15 expression may be responsible for the increased expression of SI CYP3A. To test this hypothesis, we first determined the effects of FGF19 (the human counterpart of mouse FGF15 and frequently used surrogate for FGF15 in mouse experiments; mouse FGF15 was not available for in vivo studies) on WT mice. As shown in Fig. 6A, treatment of WT mice with recombinant human FGF19 (150 μg/kg) through the tail vein for 6 hours caused significant decreases in the mRNA expression of hepatic CYP7A1 (by 76%; as a positive control) and SI CYP3A (by 61%), compared with vehicle-treated mice. The inhibitory effect of FGF19 on intestinal CYP3A expression appeared to be through direct action on the SI, as the same effect was reproduced ex vivo in cultured SI tissue; as shown in

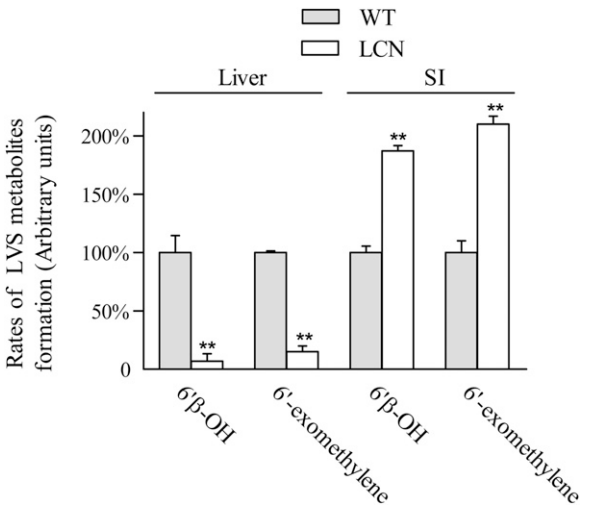

Fig. 2. In vitro metabolism of LVS by hepatic and intestinal microsomes of WT and LCN mice. Relative activities in the formation of LVS metabolites (6′β-hydroxy LVS and 6′-exomethylene LVS) were determined. Reaction mixtures contained 0.1 M potassium phosphate buffer, pH 7.4, 100 μM LVS, and 0.05 mg/ml microsomal protein in a final volume of 0.2 ml. Reactions were carried out at 37°C for 30 minutes in the presence or absence of 1.0 mM NADPH. Each microsomal preparation was obtained from pooled tissues from two to three adult female mice; three microsomal preparations were analyzed for each group. The values reported are percents of the rates determined in respective WT microsomes (means ± S.D., n = 3). **$P < 0.01$, compared with WT mice (Student's t test).

Fig. 6B, exposure of the intestine tissue to FGF19 (at 200 ng/ml, for 6 hours) decreased CYP3A expression by 30% for WT mice and by 40% for LCN mice compared with vehicle control. SI CYP3A protein expression was also decreased in vivo by FGF19 treatment, marginally in WT mice but significantly in LCN mice (by 67%, Fig. 6C). Remarkably, after FGF19 treatment, the levels of SI CYP3A protein were comparable in LCN and WT mice.

Discussion

LVS, a CYP3A substrate, was selected as a model oral drug in this study on the basis of previous findings that LVS undergoes extensive P450-mediated first-pass clearance in the SI (e.g., Zhu et al., 2011). We found that the impact of the compensatory increases in SI P450 expression on systemic clearance of orally administered LVS was dependent on LVS doses. At relatively low doses of LVS (5 and 10 mg/kg), LVS clearance was significantly increased in the LCN mice compared with WT mice, a result reflecting the dominant role of SI P450-mediated metabolism in controlling LVS bioavailability. However, the capacity of intestinal P450-mediated LVS metabolism is not unlimited. The intestinal P450 enzymes can become saturated when a sufficiently large dose of LVS is given; as a result, the relative contribution of intestinal LVS metabolism to the overall first-pass clearance of the drug would be decreased. Thus, at the higher LVS doses examined, the differences in clearance rates observed between WT and LCN mice most likely reflect the strain difference in rates of hepatic LVS metabolism.

The upregulation of CYP3A expression in the SI of LCN mice did not occur until after weaning. This time course was somewhat consistent with the time course of hepatic *Cpr* deletion, which was not complete until the mice were 2 months of age (Gu et al., 2003). Alternatively, it may reflect the role of dietary P450 inducers in this upregulation, as the regular laboratory chow may contain dietary phytochemicals that are P450 inducers. Further studies are needed to test the hypothesis that decreases in hepatic P450-mediated metabolism and elimination of dietary phytochemicals lead to their accumulation in the SI, thereby causing induction of P450 expression.

Besides CYP3A, the intestinal expression of CYP2B and CYP2C was upregulated in LCN mice relative to WT mice. The impact of the increased expression of CYP2B/2C, and possibly other xenobiotic metabolizing P450s yet to be examined, on first-pass metabolism of their substrate drugs warrants further study. A general induction of many forms of microsomal P450 enzymes was previously found to occur in the liver of the LCN or hepatic P450 reductase (POR)–null mice (Gu et al., 2003; Henderson et al., 2003) and the intestine of the IE-*Cpr*-null mice (Zhang et al., 2009). The underlying mechanism, which has been explored in several studies (Wang et al., 2005; Weng et al., 2005; Finn et al., 2009; D'Agostino et al., 2012), may be partly related to altered cellular homeostasis in tissues with the POR deficiency. In the case of the compensatory changes in SI P450s in the LCN mice, observed here, it is likely that the induction in the SI was in response to changes in cellular homeostasis resulting from loss of hepatic P450 enzyme activities that normally play a critical role in the metabolism of dietary compounds and/or in the synthesis or biotransformation of a myriad of endogenous substrates, such as BAs, that can directly or indirectly regulate SI P450 expression.

As depicted in Fig. 7, BAs are synthesized from cholesterol in the liver and transported to SI through bile. The size of the BA pool is tightly regulated within the liver and intestine to prevent accumulation of BAs and consequent cytotoxicity. Mouse FGF15 and its human counterpart FGF19 have been identified as hormones that are produced in the intestine,

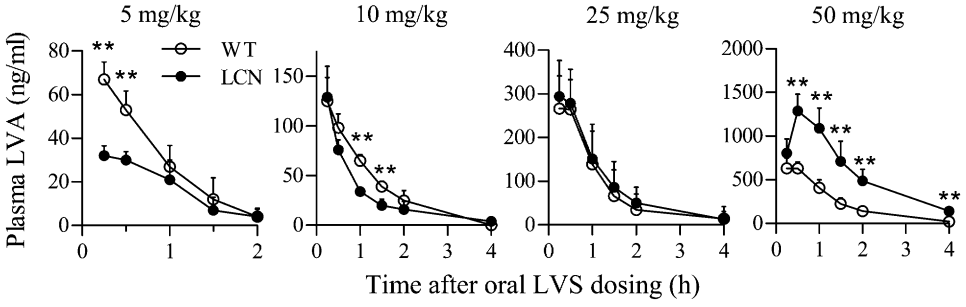

Fig. 3. In vivo clearance of LVS in LCN and WT mice. Plasma levels of LVA were determined after a single dose of LVS (5–50 mg/kg, as indicated) via oral gavage. Adult female mice were studied. Plasma samples were obtained at various times after dosing. The results shown are typical of two separate experiments. Values represent means ± S.D. (n = 5 to 6). **$P <$ 0.01; compared with WT mice (Student's t test).

TABLE 1

Pharmacokinetic parameters for plasma LVA in LCN and WT mice

Data from Fig. 3 were used for the determination of pharmacokinetic parameters, as described in *Materials and Methods*. Values represent means ± S.D. (n = 5 to 6).

Strain	Dose	T_{max}	C_{max}	$t_{1/2}$	AUC_{0-4h}	CL/F
	mg/kg	*min*	*μg/ml*	*min*	*min ·μg/ml*	*ml/min*
WT	50	27.4 ± 7.8	0.67 ± 0.11	49.6 ± 10.0	56.5 ± 8.9	18.1 ± 3.0
LCN		33.8 ± 10.6	1.30 ± 0.19*	68.2 ± 14.7**	154.5 ± 30.6*	6.7 ± 1.4*
WT	5	15.0 ± 0	0.067 ± 0.008	27.4 ± 12.2	4.1 ± 1.1	29.1 ± 9.2
LCN		20.0 ± 8.7	0.033 ± 0.004**	26.7 ± 12.8	2.1 ± 0.4**	49.4 ± 10.2

AUC, area under the curve.
*$P < 0.01$; **$P < 0.05$; compared with the corresponding WT group (Student's t test).

which are induced by BAs via activation of FXR and regulate BA homeostasis via inhibition of hepatic *Cyp7a1* transcription (Inagaki et al., 2005). A decrease in the level or activity of CYP7A1, the key enzyme in the biosynthesis of primary BAs (Myant and Mitropoulos, 1977), would reduce BA production in the liver.

Consistent with a previous report that LCN mice show drastic decreases in bile production (Henderson et al., 2003), we found large decreases in BA levels in liver, plasma, intestine, and intestinal content of the LCN mice relative to WT mice. The large decrease in BA levels in the LCN mice, presumably mainly as a result of the loss of hepatic CYP7A1 function, can perhaps explain the large decrease in the expression of FGF15 that we have observed in the SI of LCN mice. A decrease in intestinal BA levels is expected to lead to reduced activation of FXR (Hylemon et al., 2009) and consequently to result in reduced FGF15 expression (Inagaki et al., 2005). However, BAs are also known to stimulate CYP3A expression in the intestine via activation of FXR, PXR, and VDR (Xie et al.; 2001; Makishima et al., 2002; Hylemon et al., 2009). Accordingly, given the large decrease in intestinal BA levels, one would expect to see a decreased level of CYP3A expression in the intestine of LCN mice, in contrast to the upregulation of CYP3A expression that was actually observed. Therefore, the mechanisms underlying this upregulation of intestinal CYP3A expression may be more complex. Notably, the selective upregulation

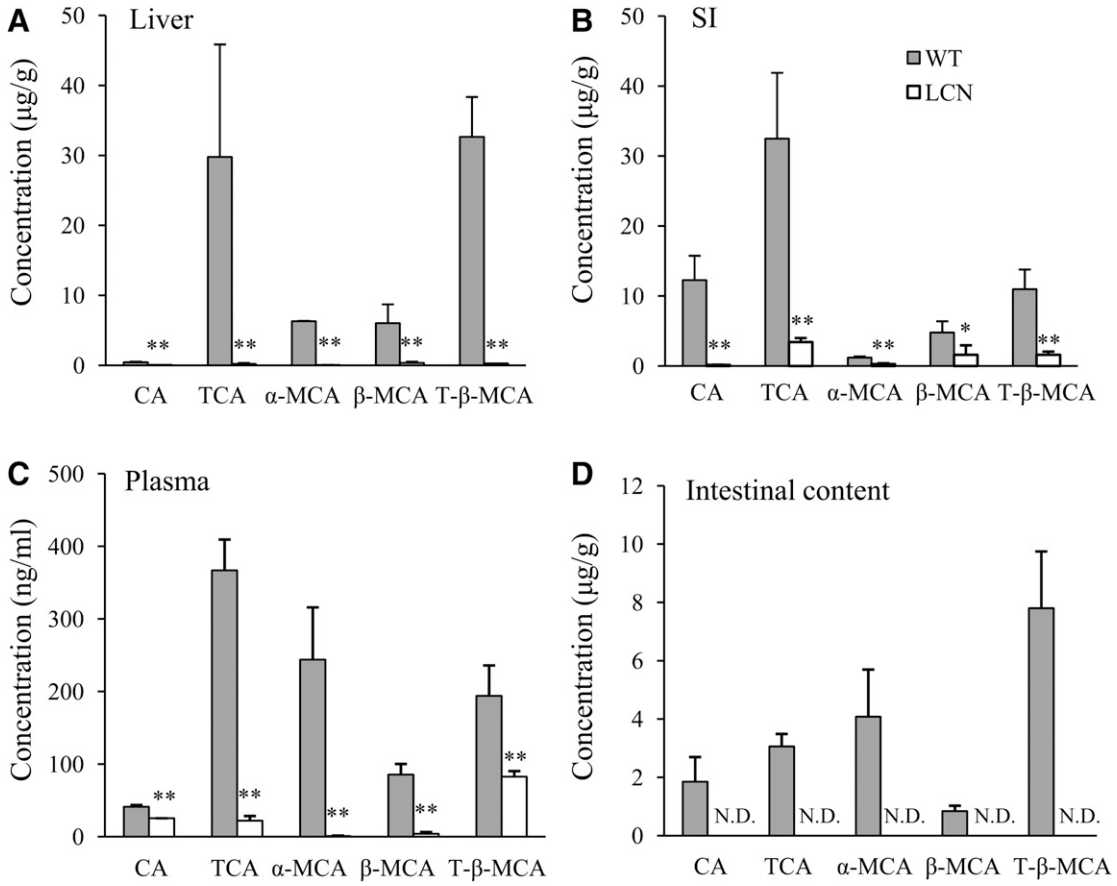

Fig. 4. BA levels in liver (A), SI epithelium (B), plasma (C), and intestinal content (D) of adult male WT and LCN mice. Five different BAs were determined using LC-MS/MS as described in *Materials and Methods*. Results are shown as means ± S.D. (n = 6). *$P < 0.05$; **$P < 0.01$, compared with WT mice (Student's t test). N.D., not detected.

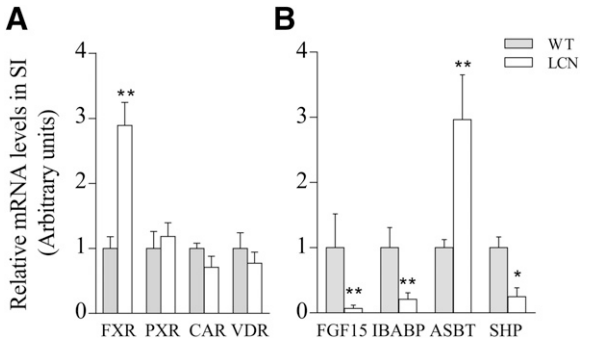

Fig. 5. RNA polymerase chain reaction (PCR) analysis of the expression of genes related with BA signaling. Levels of mRNAs for FGF15, ileal bile acid-binding protein (IBABP), ASBT, SHP (B), FXR, PXR, CAR, and VDR (A) were determined in SI for adult male WT and LCN mice. RNA-PCR was performed as described in *Materials and Methods*. RNA samples were prepared from intestinal epithelial cells of individual mice. The results are shown as relative levels in arbitrary units, with the WT group as 1 (means ± S.D; $n = 4$). *$P < 0.05$; **$P < 0.01$, compared with the corresponding WT group (Student's t test). The results are typical of three separate experiments; no sex difference was observed (data not shown).

of FXR, but not CAR, PXR, or VDR, expression in the intestine of the LCN mice suggests that FXR plays a more important role than the other receptors do in regulating bile acid homeostasis.

Our findings of the ability of FGF19 to abolish the differences in SI CYP3A expression between LCN and WT mice in vivo and the ability of FGF19 to suppress CYP3A expression ex vivo in cultured SI from both WT and LCN mice both provide strong support to the novel idea that FGF15/19 can directly suppress intestinal CYP3A expression. Thus, the large decrease in FGF15 expression in LCN SI may result in an increase in CYP3A expression, despite the decreased activation of FXR, PXR, and VDR by BA (Fig. 7). The molecular mechanism underlying the ability of FGF15/19 to regulate intestinal CYP3A expression will be an important topic for future studies. In that regard, the effects of FGF15/19 on hepatic CYP7A1 expression are mediated at least partly through the fibroblast growth factor receptor 4 and β-Klotho, which are also expressed in the mouse SI (Sinha et al., 2008; Hagiwara et al., 2009). Additionally, although the primary function of FGF15/19 in the adult is to regulate BA homeostasis in an endocrine fashion, FGF15/19 also plays a role in controlling energy homeostasis via activation of the extracellular signal-regulated kinase signaling pathway and inactivation of the transcription factor cAMP regulatory element-binding protein (Potthoff et al., 2012). Notably, FGF15/19 can regulate ASBT expression in the mouse ileum in an autocrine fashion; the mechanism of FGF15/19-mediated suppression of ASBT in the ileum was similar to that for FGF15/19-mediated suppression of CYP7A1 in the liver, as a part of the negative feedback regulation by BAs (Sinha et al., 2008). Conceivably, the regulation of CYP3A by FGF15/19 in the intestine may be via the same mechanism as for ASBT in the ileum or CYP7A1 in the liver. Thus, studies to determine whether FGFR4

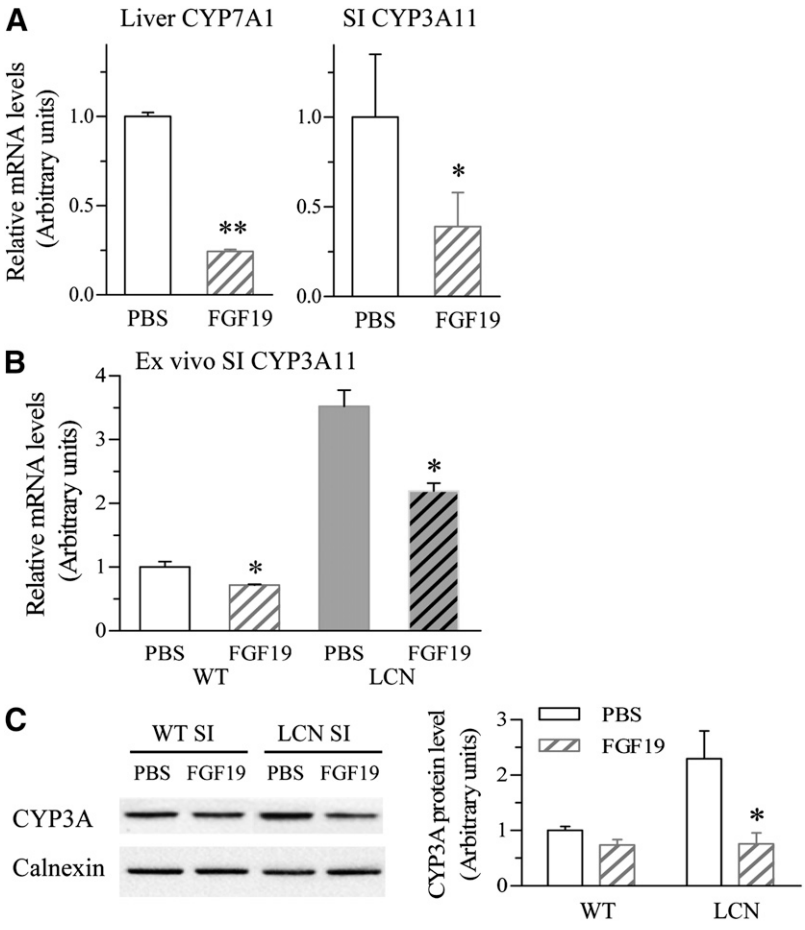

Fig. 6. Effects of FGF19 treatment on SI CYP3A and hepatic CYP7A1 gene expression in WT and LCN mice. Adult male mice were treated once with FGF19 (i.v.) at 150 μg/kg or with vehicle (PBS) alone, and liver and SI epithelial cells were obtained 6 hours later for RNA or microsome preparation and RNA polymerase chain reaction or immunoblot analysis, respectively. (A) Levels of mRNAs for hepatic CYP7A1 and SI CYP3A11 were determined for WT mice treated with PBS or FGF19. RNA samples were prepared from liver and intestinal epithelial cells of individual mice. The results are shown as relative levels in arbitrary units, with the PBS-treated group as 1 (means ± S.D.; $n = 4$). (B) Levels of mRNAs for SI CYP3A11 in ex vivo culture treated with vehicle or FGF19 (200 ng/ml) for 6 hours. SI tissue was obtained from adult WT or LCN male mice (six per group) and cultured as described in *Materials and Methods*. The results are relative levels, with the WT PBS group as 1 (means ± S.D.; $n = 6$). (C) SI microsomal proteins (20 μg) from WT and LCN mice (prepared from pooled enterocytes of two mice in each group) were analyzed for the expression of CYP3A and calnexin (loading control). Results of densitometric analysis are normalized by calnexin levels in each sample and are shown in arbitrary units. All results are typical of at least three independent experiments. *$P < 0.05$; **$P < 0.01$ compared with the corresponding PBS group (Student's t test).

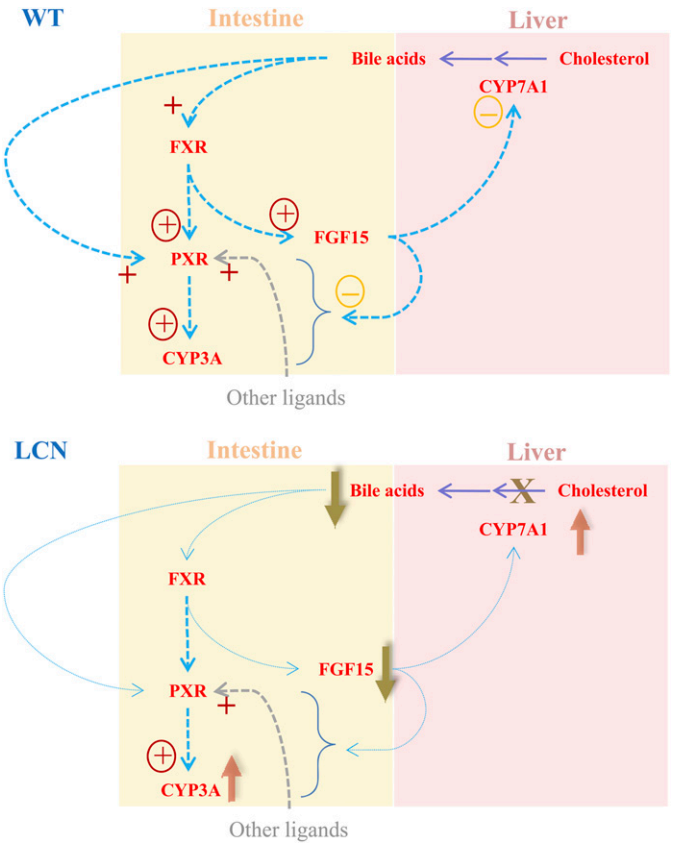

Fig. 7. Proposed scheme for a possible role of FGF15 in the regulation of SI P450 expression. In WT mice, FGF15 not only suppresses hepatic CYP7A1 expression but also somehow hinders the activation of intestinal CYP3A expression by PXR (and/or other related nuclear receptors), which is activated by both endogenous ligands such as BAs and exogenous ligands. In the LCN mice, the loss of hepatic POR/P450 function leads to blockage of the rate-limiting enzyme (CYP7A1) in BA synthesis and severe decreases in BA levels. The latter event causes large reductions in intestinal expression of FGF15, leading to upregulation of hepatic CYP7A1 expression, as well as stimulation of intestinal CYP3A expression. +, activation of receptor; "+" with circle, activation of transcription; "−" with circle, suppression of expression.

mediates the local effects of FGF15/19 on SI CYP3A expression are warranted. Furthermore, the potential involvement of other downstream or alternative mechanisms, such as activation of extracellular signal-regulated kinase and c-Jun N-terminal kinase, upregulation of PXR (or CAR/VDR) protein expression or activity, and alteration of PXR ligand availability, need to be examined.

It should be noted that our finding of compensatory increases in the expression of SI CYP2B, 2C, and 3A expression in the LCN mice is novel. Two previous reports have dealt with the relationships between liver and intestine in mice with deficient hepatic POR expression (Mutch et al., 2006, 2007), but neither study reported comparisons of the constitutive expression or activity of intestinal drug-metabolizing CYPs between wild-type and hepatic POR-null mice. The microarray data in the more recent study (Mutch et al., 2007) did show a modest increase in *Fxr* expression in the ileum of the hepatic POR-null mice, relative to that in WT mice, a finding confirmed here by RNA polymerase chain reaction analysis in the LCN mice. Together, these studies provide strong support for the notion that gene expression in the liver and intestine is coordinately regulated in response to environmental perturbation or genetic deficiency.

In summary, we have shown that loss of hepatic P450/CPR activity, as occurs in LCN mice, leads to increases in the expression of multiple SI drug-metabolizing P450 enzymes, with consequent increases in the first-pass clearance of a commonly prescribed oral drug, LVS. Our findings suggest that human patients with compromised hepatic P450/CPR function may also have compensatory increases in drug-metabolism capacity in the SI and may thus experience decreases in the bioavailability (and thus efficacy) of an oral drug or else elevated risks of drug-induced toxicity in the SI. Our initial efforts toward identification of the underlying mechanisms uncovered evidence in strong support of the novel idea that intestinal FGF15/19 can regulate SI CYP3A expression in response to changes in BA homeostasis. Taken together, our results not only shed new light on physiologic regulation of SI P450 expression but will also help with data interpretation for numerous studies utilizing the LCN mouse model to determine roles of hepatic P450s in the disposition of orally administered drugs and with prediction of drug exposure in patients with compromised hepatic P450 function as a result of diseases or genetic defects.

Acknowledgments

The authors thank Drs. Xin Zhou and Jaime D'Agostino for help with the development of the LC-MS/MS method, Dr. Peng Zhang for BA analysis, and Weizhu Yang for mouse production.

Authorship Contributions

Participated in research design: Zhu, Ding, Fang, Zhang.
Conducted experiments: Zhu, Fang, Zhang.
Performed data analysis: Zhu, Ding, Zhang.
Wrote or contributed to the writing of the manuscript: Zhu, Ding, Zhang.

References

Cariou B, van Harmelen K, Duran-Sandoval D, van Dijk TH, Grefhorst A, Abdelkarim M, Caron S, Torpier G, Fruchart JC, and Gonzalez FJ et al. (2006) The farnesoid X receptor modulates adiposity and peripheral insulin sensitivity in mice. *J Biol Chem* **281**:11039–11049.

D'Agostino J, Ding X, Zhang P, Jia K, Fang C, Zhu Y, Spink DC, and Zhang QY (2012) Potential biological functions of cytochrome P450 reductase-dependent enzymes in small intestine: novel link to expression of major histocompatibility complex class II genes. *J Biol Chem* **287**:17777–17788.

Duggan DE, Chen IW, Bayne WF, Halpin RA, Duncan CA, Schwartz MS, Stubbs RJ, and Vickers S (1989) The physiological disposition of lovastatin. *Drug Metab Dispos* **17**:166–173.

Fang C, Behr M, Xie F, Lu S, Doret M, Luo H, Yang W, Aldous K, Ding X, and Gu J (2008) Mechanism of chloroform-induced renal toxicity: non-involvement of hepatic cytochrome P450-dependent metabolism. *Toxicol Appl Pharmacol* **227**:48–55.

Fasco MJ, Silkworth JB, Dunbar DA, and Kaminsky LS (1993) Rat small intestinal cytochromes P450 probed by warfarin metabolism. *Mol Pharmacol* **43**:226–233.

Finn RD, Henderson CJ, Scott CL, and Wolf CR (2009) Unsaturated fatty acid regulation of cytochrome P450 expression via a CAR-dependent pathway. *Biochem J* **417**:43–54.

Froicu M, Zhu Y, and Cantorna MT (2006) Vitamin D receptor is required to control gastrointestinal immunity in IL-10 knockout mice. *Immunology* **117**:310–318.

Gu J, Chen CS, Wei Y, Fang C, Xie F, Kannan K, Yang W, Waxman DJ, and Ding X (2007) A mouse model with liver-specific deletion and global suppression of the NADPH-cytochrome P450 reductase gene: characterization and utility for in vivo studies of cyclophosphamide disposition. *J Pharmacol Exp Ther* **321**:9–17.

Gu J, Weng Y, Zhang QY, Cui H, Behr M, Wu L, Yang W, Zhang L, and Ding X (2003) Liver-specific deletion of the NADPH-cytochrome P450 reductase gene: impact on plasma cholesterol homeostasis and the function and regulation of microsomal cytochrome P450 and heme oxygenase. *J Biol Chem* **278**:25895–25901.

Hagiwara A, Nakayama F, Motomura K, Asada M, Suzuki M, Imamura T, and Akashi M (2009) Comparison of expression profiles of several fibroblast growth factor receptors in the mouse jejunum: suggestive evidence for a differential radioprotective effect among major FGF family members and the potency of FGF1. *Radiat Res* **172**:58–65.

Henderson CJ, Otto DM, Carrie D, Magnuson MA, McLaren AW, Rosewell I, and Wolf CR (2003) Inactivation of the hepatic cytochrome P450 system by conditional deletion of hepatic cytochrome P450 reductase. *J Biol Chem* **278**:13480–13486.

Hylemon PB, Zhou H, Pandak WM, Ren S, Gil G, and Dent P (2009) Bile acids as regulatory molecules. *J Lipid Res* **50**:1509–1520.
Inagaki T, Choi M, Moschetta A, Peng L, Cummins CL, McDonald JG, Luo G, Jones SA, Goodwin B, and Richardson JA et al. (2005) Fibroblast growth factor 15 functions as an enterohepatic signal to regulate bile acid homeostasis. *Cell Metab* **2**:217–225.
Ishigami M, Honda T, Takasaki W, Ikeda T, Komai T, Ito K, and Sugiyama Y (2001) A comparison of the effects of 3-hydroxy-3-methylglutaryl-coenzyme a (HMG-CoA) reductase inhibitors on the CYP3A4-dependent oxidation of mexazolam in vitro. *Drug Metab Dispos* **29**:282–288.
Kim I, Ahn SH, Inagaki T, Choi M, Ito S, Guo GL, Kliewer SA, and Gonzalez FJ (2007) Differential regulation of bile acid homeostasis by the farnesoid X receptor in liver and intestine. *J Lipid Res* **48**:2664–2672.
Lodge JW, Fletcher BL, Brown SS, Parham AJ, Fernando RA, and Collins BJ (2008) Determination of lovastatin hydroxy acid in female B6C3F1 mouse serum. *J Anal Toxicol* **32**:248–252.
Makishima M, Lu TT, Xie W, Whitfield GK, Domoto H, Evans RM, Haussler MR, and Mangelsdorf DJ (2002) Vitamin D receptor as an intestinal bile acid sensor. *Science* **296**:1313–1316.
Miyata M, Yamakawa H, Hamatsu M, Kuribayashi H, Takamatsu Y, and Yamazoe Y (2011) Enterobacteria modulate intestinal bile acid transport and homeostasis through apical sodium-dependent bile acid transporter (SLC10A2) expression. *J Pharmacol Exp Ther* **336**:188–196.
Mutch DM, Crespy V, Clough J, Henderson CJ, Lariani S, Mansourian R, Moulin J, Wolf CR, and Williamson G (2006) Hepatic cytochrome P-450 reductase-null mice show reduced transcriptional response to quercetin and reveal physiological homeostasis between jejunum and liver. *Am J Physiol Gastrointest Liver Physiol* **291**: G63–G72.
Mutch DM, Klocke B, Morrison P, Murray CA, Henderson CJ, Seifert M, and Williamson G (2007) The disruption of hepatic cytochrome p450 reductase alters mouse lipid metabolism. *J Proteome Res* **6**:3976–3984.
Myant NB and Mitropoulos KA (1977) Cholesterol 7 alpha-hydroxylase. *J Lipid Res* **18**:135–153.
Patel RD, Hollingshead BD, Omiecinski CJ, and Perdew GH (2007) Aryl-hydrocarbon receptor activation regulates constitutive androstane receptor levels in murine and human liver. *Hepatology* **46**:209–218.
Potthoff MJ, Kliewer SA, and Mangelsdorf DJ (2012) Endocrine fibroblast growth factors 15/19 and 21: from feast to famine. *Genes Dev* **26**:312–324.
Schmidt DR, Holmstrom SR, Fon Tacer K, Bookout AL, Kliewer SA, and Mangelsdorf DJ (2010) Regulation of bile acid synthesis by fat-soluble vitamins A and D. *J Biol Chem* **285**:14486–14494.
Sinha J, Chen F, Miloh T, Burns RC, Yu Z, and Shneider BL (2008) beta-Klotho and FGF-15/19 inhibit the apical sodium-dependent bile acid transporter in enterocytes and cholangiocytes. *Am J Physiol Gastrointest Liver Physiol* **295**:G996–G1003.
Trousson A, Makoukji J, Petit PX, Bernard S, Slomianny C, Schumacher M, and Massaad C (2009) Cross-talk between oxysterols and glucocorticoids: differential regulation of secreted phopholipase A2 and impact on oligodendrocyte death. *PLoS ONE* **4**:e8080.
Wang XJ, Chamberlain M, Vassieva O, Henderson CJ, and Wolf CR (2005) Relationship between hepatic phenotype and changes in gene expression in cytochrome P450 reductase (POR) null mice. *Biochem J* **388**:857–867.
Weng Y, DiRusso CC, Reilly AA, Black PN, and Ding X (2005) Hepatic gene expression changes in mouse models with liver-specific deletion or global suppression of the NADPH-cytochrome P450 reductase gene: mechanistic implications for the regulation of microsomal cytochrome P450 and the fatty liver phenotype. *J Biol Chem* **280**:31686–31698.
Xie W, Radominska-Pandya A, Shi Y, Simon CM, Nelson MC, Ong ES, Waxman DJ, and Evans RM (2001) An essential role for nuclear receptors SXR/PXR in detoxification of cholestatic bile acids. *Proc Natl Acad Sci USA* **98**:3375–3380.
Zhang P, Jia K, Fang C, Zhou X, Ding X, and Zhang QY (2013) Dietary regulation of mouse intestinal P450 expression and drug metabolism. *Drug Metab Dispos* **41**:529–535.
Zhang QY, Dunbar D, and Kaminsky LS (2003) Characterization of mouse small intestinal cytochrome P450 expression. *Drug Metab Dispos* **31**:1346–1351.
Zhang QY, Fang C, Zhang J, Dunbar D, Kaminsky L, and Ding X (2009) An intestinal epithelium-specific cytochrome P450 (P450) reductase-knockout mouse model: direct evidence for a role of intestinal p450s in first-pass clearance of oral nifedipine. *Drug Metab Dispos* **37**:651–657.
Zhang QY, Kaminsky LS, Dunbar D, Zhang J, and Ding X (2007) Role of small intestinal cytochromes p450 in the bioavailability of oral nifedipine. *Drug Metab Dispos* **35**:1617–1623.
Zhu Y, D'Agostino J, and Zhang QY (2011) Role of intestinal cytochrome P450 (P450) in modulating the bioavailability of oral lovastatin: insights from studies on the intestinal epithelium-specific P450 reductase knockout mouse. *Drug Metab Dispos* **39**:939–943.
Zhu Y and Zhang QY (2012) Role of intestinal cytochrome p450 enzymes in diclofenac-induced toxicity in the small intestine. *J Pharmacol Exp Ther* **343**:362–370.

Address correspondence to: Dr. Qing-Yu Zhang, Wadsworth Center, New York State Department of Health, Empire State Plaza, Box 509, Albany, NY 12201-0509. E-mail: zhangq@wadsworth.org